

Thin film silicon solar cell design based on photonic crystal and diffractive grating structures

James G. Mutitu, Shouyuan Shi, Caihua Chen, Timothy Creazzo, Allen Barnett,
Christiana Honsberg and Dennis W. Prather

Dept of Electrical and Computer Engineering, University of Delaware, 151 Evans Hall Newark, Delaware 19716
mutitu@mail.eecis.udel.edu
<http://www.ece.udel.edu/>

Abstract: In this paper we present novel light trapping designs applied to stand alone and multiple junction thin film silicon solar cells. The new designs incorporate one dimensional photonic crystals as band pass filters that reflect short light wavelengths (400 – 1100 nm) and transmit longer wavelengths (1100 -1800 nm) at the interface between two adjacent cells. In addition, nano structured diffractive gratings that cut into the photonic crystal layers are incorporated to redirect incoming waves and hence increase the optical path length of light within the solar cells. Two designs based on the nano structured gratings that have been realized using the scattering matrix and particle swarm optimization methods are presented. We also show preliminary fabrication results of the proposed light trapping grating structures.

© 2008 Optical Society of America

OCIS codes: (350.6050) Solar energy; (310.6805) Theory and design; (050.5298) Photonic crystals; (310.6845) Thin film devices and applications.

References and links

1. T. Markvart, *Solar Electricity* 2nd Ed., (John Wiley and Sons, 2000).
2. M. A. Green, *Third Generation Photovoltaics: Advanced Solar Energy Conversion* (Springer, 2003).
3. A. Barnett, C. Honsberg, D. Kilpatrick, et.al., "50% Efficient Solar Cell Architectures and Designs," in *Conference Record of the IEEE 4th World Conference on Photovoltaic Energy Conversion*. (Waikoloa, Hawaii, 2006), pp. 2560 – 2564.
4. K. Yamamoto, "Thin-film crystalline Silicon solar cell." *JSAP Int.* **7**, 12-19 (2003).
5. A. V. Shah, H. Schade, M. Vanecek, and J. Meier, "Thin-Film Silicon Solar Cell Technology," *Prog. Photovoltaics* **12**, 113 - 142 (2004).
6. S. Hegedus, "Thin Film Solar Modules: The Low Cost, High Throughput and Versatile Alternative to Si Wafers," *Prog. Photovoltaics* **14**, 393–411 (2006).
7. M. J. McCann, K. R. Catchpole, K. J. Weber, and A. W. Blakers, "A review of thin-film crystalline silicon for solar cell applications. Part 1: Native substrates," *Sol. Energy Mater. Sol. Cells* **68**, 135-171(2001).
8. K. R. Catchpole, M. J. McCann, K. J. Weber, A. W. Blakers, "A review of thin-film crystalline silicon for solar cell applications. Part 2: Foreign substrates," *Sol. Energy Mater. Sol. Cells* **68**, 173-215 (2001).
9. H. A. Macleod, *Thin-Film Optical Filters*, (Adam Hilger Ltd, 1986).
10. J. Muller, B. Rech, J. Springer, and M. Vanecek, "TCO and light trapping in silicon thin film solar cells," *Sol. Energy* **77**, 917–930 (2004).
11. D. H. Macdonald, A. Cuevas, M. J. Kerr, C. Samundsett, D. Ruby, S. Winderbaum and A. Leo, "Texturing industrial multicrystalline silicon solar cells," *Sol. Energy* **76**, 277–283 (2004).
12. M. A. Green, *Solar Cells: operating principles, technology, and system applications* (Prentice Hall, 1982).
13. J. Zhao, A. Wang and M. A. Green, "19.8% efficient "honeycomb" textured multicrystalline and 24.4% monocrystalline silicon solar cells," *Appl. Phys Letts* **73**, 1991-1993 (1998).
14. E. Yablonovitch and G. Cody, "Intensity Enhancement in Textured Optical Sheets," *IEEE Trans. Electron. Devices* **29**, 300-305 (1982).
15. A. C. Marsh and J. C Inkson, "Scattering matrix theory of transport in heterostructures," *Semicond. Sci. Technol.* **1**, 285 – 290, (1986).

16. J. Yonekura, M. Ikeda, and T. Baba, "Analysis of Finite 2-D Photonic Crystals of Columns and Lightwave Devices using the Scattering Matrix Method," *J. Lightwave Technol.* **17**, 1500-1508, (1999).
17. Q. Wang, Y. Zhang, and B. Ooi, E. Li "Analysis of Finite-Size Coated Electromagnetic Band gap Structure by an Efficient Scattering Matrix Method," *IEEE J. Sel. Top. Quantum Electron* **11**, 485-492 (2005).
18. R. Eberhart and J. Kennedy, "A new optimizer using particle swarm theory," in *Proceedings of the Sixth International Symposium on Micromachine and Human Science*, (Academic, Nagoya, Japan. 1995) pp. 39-43.
19. R. Eberhart and Y. Shi, "Particle swarm optimization: developments, applications and resources," in *Proceedings of the 2001 Congress on Evolutionary Computation*, (Academic, Seoul, South Korea. 2001) pp. 81-86.
20. J. M. Gee "Optically enhanced absorption in thin silicon layers using photonic crystals," in *Proceedings of 29th IEEE Photovoltaic Specialists Conference* (Institute of Electrical and Electronics Engineers, New Orleans, LA, 2002), pp. 150 – 153.
21. L. Zeng, Y. Yi, C. Hong, B. Alamri, J. Liu, X. Duan, and L. Kimerling, "New Solar Cells with Novel Light Trapping via Textured Photonic Crystal Back Reflector," in *Mater. Res. Soc. Symp. Proc. Vol. 891*, (Material Research Society, 2006).
22. L. Zeng, Y. Yi, C. Hong, J. Liu, X. Duan and L. Kimerling, "Efficiency enhancement in Si solar cells by textured photonic crystal back reflector," *Appl. Phys. Lett.* **89**, 111111 (2006).
23. N. Feng, J. Michel, L. Zeng, J. Liu, C. Hong and L. Kimerling, "Design of Highly Efficient Light-Trapping Structures for Thin-Film Crystalline Silicon Solar Cells," *IEEE Trans. Electron. Devices* **54**, 1926-1933 (2007).
24. P. Bermel, C. Luo, L. Zeng, L. C. Kimerling, and J. D. Joannopoulos, "Improving thin-film crystalline silicon solar cell efficiencies with photonic crystals," *Opt. Express* **15**, 16986-17000 (2007).
25. X. Hu, *Particle Swarm Optimization*, (Swarm Intelligence, 2006). <http://www.swarmintelligence.org/>
26. R. Brendel, *Thin-Film Crystalline Silicon Solar Cells* (Wiley-VCH, 2003), Chaps.1 and 2.
27. D. W. Prather, A. Sharkawy, and S. Shi, *Design and Applications of Photonic Crystals*, 2nd ed. (CRC Press, "Nanotechnology Handbook," to appear 2007).
28. S. Venkataraman, "Fabrication of Two-Dimensional and Tree-Dimensional Photonic Crystal Devices for Applications in Chip-Scale Optical interconnects" (PhD dissertation, University of Delaware, 2005).
29. C. Heine, "Submicrometer gratings for solar energy applications." *Appl. Opt.* **34**, 2476- 2482 (1995).
30. J. D. Joannopoulos, S. G. Johnson, J. N. Winn and R. D. Meade, *Photonic Crystals: Molding the Flow of Light*, Second ed. (Princeton: Princeton University Press, 2008), Chap. 4.

1. Introduction

There are many avenues being explored to improve the efficiencies and reduce the costs of solar cells. One of the candidates in this endeavor has been thin film solar cells, which offer solutions in terms of cost reduction. However, low cell efficiencies, 5-11% for commercial products, 16% for the best research cells [1], and recombination losses still prove to be major challenges that thin film devices face. In light of these issues, we consider high efficiency cells that can function well as both stand alone devices and elements in a multi device stack as viable solutions [2]. In the case of the multi device stack arrangements we design cells that would fit into both the lateral architecture and the independently contacted vertical junction stack that was presented by Barnett et al [3]. In the lateral architecture, incident light is split into spectral components that are then diverted to cells of different band gap energies. In the vertical stack approach, high energy cells are stacked on top of lower band gap cells, hence only the energy that is unabsorbed by cells higher up in the stack trickles down to the low energy cells. We design silicon cells that would function well as mid band gap energy cells in both architectures. In the lateral case the light would be split in a way that only bandwidths unabsorbed by higher energy cells would be incident on our mid energy silicon cells. In the vertical junction stack our silicon cell would be placed below a Gallium Arsenide cell (with band gap of 1.43 eV). For our cells to function well as both single junction and as elements in the aforementioned architectures, we first optimize the light trapping parameters for the 400 – 1100 nm wavelength range. We then consider the enhancement factor in the 867 – 1100 nm range because this would be the band of available incident light on our silicon solar cells when placed in the aforementioned architectures. Finally we analyze the short circuit characteristics of our designs as compared to non modified cells in the full 400 – 1100 nm range to establish their viability as stand alone devices.

Thin film devices with efficient light trapping schemes have a number of advantages. First, the amount of high quality silicon needed in manufacturing each solar cell is significantly reduced. Second, the reduction in cell thickness improves the collection efficiency of electron-hole pairs [4, 5]. Third, thin film technology offers prospects for reducing material losses, especially the apparent losses of high quality silicon as sawdust from CZ grown ingots. To this end, many thin film deposition techniques are being investigated [6 - 8], which will ultimately reduce the overall costs by eliminating the cost of silicon wafers. Finally, thin film technology has the added advantage of increasing the size of the unit of manufacturing, i.e., the unit size is not constrained to the area of a silicon wafer [2].

Light trapping in silicon solar cells mainly falls into two categories, the first being the reduction of front surface reflection and the second involves increasing the optical path length of light within the cell. The concept of reducing the surface reflectivity by introducing intermediate transparent layers has been known since the early 1800's [8]. These intermediate layers serve to 'buffer' the drastic refractive index changes between low index and higher index materials. Combinations of materials, such as silicon dioxide (SiO_2), silicon nitride (Si_3N_4) and some transparent conductive oxides [9, 10] are commonly used as the intermediate layers. Other methods used to reduce front surface reflection are based on principles of scattering and impedance matching and they range from random surface texturing [10] to the use of regularly arrayed or inverted pyramidal structures [11-13].

The second aforementioned category, i.e., increasing the optical path length of light within the device, involves the modification of both the front and back surfaces of the device. To accomplish this, numerous ideas and designs have emerged ranging from planar reflective surfaces to arrays of ordered nano structures integrated on the back surface. The main aim behind these designs is to totally internally reflect incoming light and hence increase the effective thickness towards a maximum factor of $4n^2$ for indirect band gap semiconductors [15] such as crystalline silicon (effective thickness of silicon increases to 50), which our designs are based on.

In our study we combine planar AR coatings with nano structured diffractive gratings to enhance the light trapping capabilities of the solar cells and hence increase the short circuit current characteristics of the device. To model the devices we employ the scattering matrix method [15-17] and particle swarm optimization algorithm [18, 19]. We focus on 5 micron silicon solar cells in this paper, mainly as a starting point towards investigating ultra thin films of thicknesses that are less than 5 microns; they all have poor absorption characteristics close to the silicon band edge. When calculating the short circuit current we assume the internal quantum efficiency to be unity and do not consider the internal carrier collection efficiency; we consider only optical loss parameters.

In designing an element of a multi device stack one has to take into account the performance of subsequent devices and hence accommodate some of the constraints the situation presents, such as having no back surface reflectors for elements in the stack. To solve this problem we use a one dimensional photonic crystal (1D-PhC) engineered to reflect and transmit the desired bandwidths. We then cut symmetric and periodic groves into the 1D-PhC layers to form diffractive gratings. This design technique utilizes the beam redirecting property of the grating while still maintaining the selective characteristics of the 1D-PhC. Early work on the incorporation of photonic crystals into solar cells to enhance light trapping was performed by James Gee [20] who put forth the idea that the statistical limit for optical enhancement, shown by Yablonovitch [14] to be $4n^2$ (where n is the refractive index of the material - about 50 for silicon), could be surpassed over a narrow spectral and angular range using photonic band gap materials. More recently several groups have also been working on combining photonic crystals with gratings to enhance the light trapping capabilities of solar cells [21-24]. The novelties of our designs lie in our fundamental approach to designing solar cells that can function both as stand alone cells or part of multiple device stacks. We consider the transmission characteristics of the devices to be important and hence we design the

photonic crystals to simultaneously reflect shorter wavelengths (400 – 1100 nm) back into the silicon cell and transmit longer wavelengths (1100 – 1800nm) to underlying lower energy cells. In addition, we cut through the layers of the 1D-PhC stack to generate our gratings and are hence able to seamlessly combine the diffractive and reflective properties of the gratings for optimal optical path length enhancement.

2. Modeling and analysis

Due to the sub wavelength feature sizes associated with the nano structured gratings a rigorous electromagnetic simulation tool is required and hence we opt to use the scattering matrix (S-Matrix) algorithm [15-17]. The S-Matrix method is also able to incorporate lossy (even in metallic materials) and dispersive (frequency dependent) materials. In addition, the S-Matrix method when used with multiple stacked layers, regardless of the thickness of each layer, is more efficient than volumetric numerical electromagnetic techniques such as the finite element method or the finite difference time domain method. When the S-Matrix method is applied to grating structures the field along the lateral direction may be expanded using a Fourier series and as a result, the diffraction orders can be easily determined [14 -16].

For optimization we use the Particle Swarm Optimization (PSO) method which is a population based stochastic optimization technique that derives inspiration from the ‘swarming’ behavior of various life forms, e.g., a flock of birds [25]. The basic function of the PSO algorithm is as follows: the system is initialized by assigning random population positions and velocities in the problem space. Potential solutions called particles are also initialized in the problem space. The fitness of each individual particle is then calculated. Each particle keeps track of its position in the problem space which is associated with its highest fitness position namely the local best. The best position within all populations is called the global best. So at each time step each particle’s velocity is compared to the local best and the global best and then each particle is accelerated towards the local best and the global best positions. We then loop back to the second step, i.e., evaluating the fitness of each individual particle [18, 19].

The equations behind the PSO algorithm can be understood as the changing of the velocity V_i (accelerating) of each particle (entity in the swarm) P_i toward a space of the highest ‘fitness’ value s_i and the global best, g_i , locations. The basic loop can be summarized by the following equations [18, 19]:

$$\begin{aligned} V_{i+1} &= V_i + c_1 \text{rand}(s_i - P_i) + c_2 \text{rand}(g_i - P_i) \\ P_{i+1} &= P_i + V_{i+1}, \end{aligned} \quad (1)$$

where $\text{rand}()$ is a random number generating function that outputs a random value between zero and one.

To calculate the fitness of each position in the space we define a figure of merit function that takes into account both absorption and transmission characteristics at different bandwidths as shown below:

$$\begin{aligned} MF &= \int_{\lambda=400}^{\lambda=1100} [(1 - A(\lambda')) \text{Irrd}(\lambda')]^2 + [T(\lambda') \text{Irrd}(\lambda')]^2 d\lambda' \\ &+ \int_{\lambda=1100}^{\lambda=1800} [(1 - T(\lambda')) \text{Irrd}(\lambda')]^2 + [A(\lambda') \text{Irrd}(\lambda')]^2 d\lambda' \end{aligned} \quad (2)$$

where A is the absorption, T is the transmission and Irrd is the solar irradiance spectra.

The PSO algorithm is fast and with few adjustable parameters and therefore finds numerous applications in the optimization of non linear functions [18, 19, 25].

We define a new quantity for band edge enhancement, the enhancement factor (EF), as the ratio of the average absorption of a modified silicon solar cell to the average absorption of a silicon cell with no light trapping structures (no AR coating). We calculate the absorption of an enhanced structure for a given spectrum range near the band edge (1100 nm) and normalize it to the absorption characteristics of a cell without any light trapping structures as shown in Eq. (3) below.

$$EF(\lambda) = \frac{\int_{\lambda}^{\lambda=1100} A_E(\lambda') Irrd(\lambda') d\lambda'}{\int_{\lambda}^{\lambda=1100} A_s(\lambda') Irrd(\lambda') d\lambda'} , \quad (3)$$

where the value A_E represents the absorption characteristics of an enhanced structure, i.e., with the AR coating at the top surface and light trapping structures at the bottom surface, A_s represents the absorption of a silicon structure with no light trapping structures at the top or bottom surfaces (no AR coating). When calculating the enhancement factor, we take 1100 nm as the upper limit of integration and for the lower limit we specify a wavelength whose interval with the upper limit defines the domain of integration which specifies the enhancement region and hence the EF is a function of the wavelength. In our study, we are interested in the silicon band edge enhancement, i.e., in the 867 – 1100 nm range for this is where silicon has, due to its indirect band gap, poor intrinsic absorption particularly in thin film solar cells. In addition this band corresponds to the wavelengths that are available to be absorbed by our silicon cell when applied to the multi device architectures described by Barnett et al [3] i.e. light available after being split or passing down from a GaAs cell.

We use Eq. (4). below to calculate the short circuit current characteristics of the solar cells [26].

$$J_{sc} = \frac{q}{hc} \int_{\lambda}^{\lambda=1100} \lambda' A(\lambda') Irrd(\lambda') d\lambda' , \quad (4)$$

where J_{sc} is the short circuit current density, q is the charge on an electron, h is Planck's constant, c is the speed of light, λ is the wavelength, A is the absorption characteristic of the silicon structure and $Irrd$ is the solar irradiance spectrum.

3. Designs of silicon cells

Using the aforementioned modeling techniques we design silicon solar cells that absorb light energy within the 400 – 1100 nm bandwidth while transmitting light with wavelengths above 1100 nm to other cells in the multiple device stack, as shown in Fig. 1. We assume that the light is incident normally on the top surface of the solar cells. To optimize the transmission as well as enhance optical path length we use a 1D-PhC combined with various diffractive gratings. The 1D-PhC is designed to behave as a selective light filter that reflects light with wavelengths below 1100 nm and transmits light with wavelengths greater than 1100 nm. This arrangement enhances the light trapping capabilities of the silicon solar cell while allowing longer wavelengths to transmit to subsequent low energy cells thus increasing the efficiency of the silicon cell and overall multi device arrangement. This type of design i.e. a selective light filter with incorporated diffractive gratings can also be applied to cells of higher or lower energy than silicon in the same multi device stack. We restricted the thickness of each design to 5 microns hence qualifying our designs as thin film silicon solar cells; thin film crystalline silicon solar cells are defined as having cell thicknesses of less than 50 microns. The short circuit current limit for a 5 micron device is 39.7 mA/cm² [26].

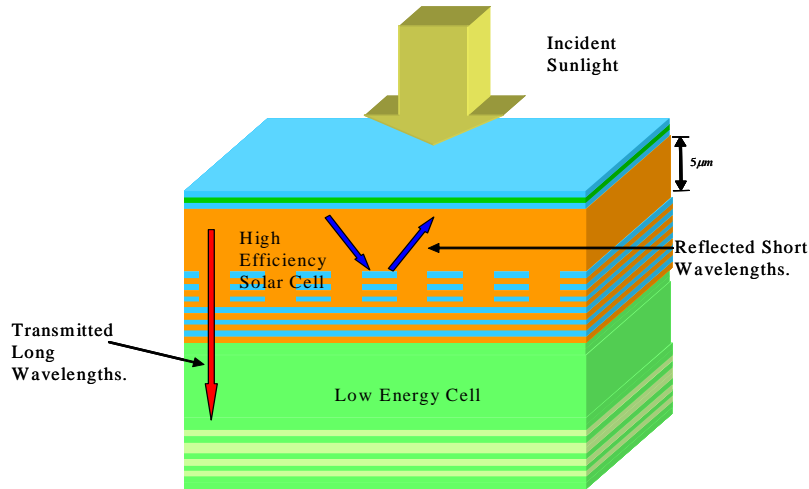


Fig. 1. Schematic diagram showing a multiple junction solar cell with the short wavelengths being reflected back into the first cell and long wavelengths being transmitted to the lower energy solar cells.

A photonic crystal is a periodic arrangement of dielectric or metallic material with a lattice constant comparable to the wavelength of an electromagnetic wave. In the construction of the 1D-PhC, alternating layers of material with different refractive indices are stacked to form a structure that is periodic along one direction. The parameters that determine the band structure are the refractive index contrast and thicknesses of the constituting layers. A distributed-Bragg reflector is a good example of a 1D-Phc [27, 28]. We use nano structured diffractive gratings to increase the optical path length of light within the solar cell. In our study we consider binary and triangular gratings. We choose these gratings because they are relatively easy to fabricate as compared to other grating structures such as blazed gratings. We also choose them because they are polarization insensitive. In a binary grating both positive and negative diffraction orders are reflected from the surface of the grating with the same magnitude. If the diffraction angle is greater than the critical angle, total internal reflection occurs. However, by the reciprocity theorem, the totally internally reflected wave impinges on the surface of the grating in the same way it is generated. Hence, it couples to an outgoing zero order wave that reflects off the surface of the grating and gets lost from the solar cell [29]. To minimize this phenomenon we considered a triangular grating which, when used in conjunction with a second grating (binary) placed on the top surface of the solar cell (below the AR coating), introduces an angular shift in the reflected waves and hence helps to suppress lower order modes.

The first device we present includes a triple layer planar AR coating on the front surface and a diffractive binary grating coupled into a 1D-PhC on the back surface. The AR coating consists of a layer of Si_3N_4 embedded between two layers of SiO_2 with the layer nearest the silicon being primarily for the purpose of passivation. Figure 2(a) is the schematic diagram of the model with an inset scanning electron microscope (SEM) image of the fabricated grating and an inset expanded representation of the grating. The fabrication methodology used to realize the grating is divided into several steps comprised primarily of plasma enhanced chemical vapor deposition (PECVD), electron beam (E-beam) lithography, and inductively coupled plasma (ICP) etching. The one dimensional photonic crystal layers are deposited by PECVD. The pattern for the diffraction grating in the upper layers of the 1-D photonic crystal

is generated using E-beam lithography and transferred with an ICP etching process. Figure 2(b) shows the simulated short circuit current characteristics of the designed structure. The enhanced design is compared to a base case that consists of a bare silicon slab with no light trapping and also to the ideal case where the short circuit current is maximum. To optimize the light trapping characteristics we optimized the thicknesses of the AR coating, the alternating photonic crystal layers, and for the grating we considered the period and duty cycle as design parameters. We obtained optimal results for AR coating thicknesses of 98 nm for the top SiO₂ layer and 48 nm for the Si₃N₄ layer with the third SiO₂ layer fixed at 8nm. The optimal grating period is 970 nm, the duty cycle is 0.5 and the thicknesses of the six photonic crystal alternating (Si and SiO₂) layers is 128 nm for the SiO₂ layers and 218 nm for the silicon layers as shown in Fig. 2(a). Thus the grating depth is 1038 nm (three alternating layers); the entire 1D-PhC stack consisted of six alternating layers with the first three etched through to form the grating and the three others below the grating. The large contrast in refractive index between SiO₂ and Si provides a bandgap based on photonic bandgap material designs. The thickness of each layer is hence not necessarily a quarter wavelength ($\lambda/4n$ where λ is the wavelength in free space and n is the refractive index of the material). The alternating layer thickness is calculated as an optimization design parameter hence the thickness of layers is the optimal thickness for accomplishing the task of reflecting 400 – 1100 nm light and transmitting 1100 – 1800 nm light [30].

This new design augments the reflective and diffractive properties of the grating, which in turn improves the band edge absorption. This device absorbs 71 % (400 – 1100 nm) of the incident energy, which results in a short circuit current (400 – 1100 nm) of 27.4 mA/cm², a band edge (867 -1100nm) enhancement factor of 3.9 and transmission of 54% of the total energy within the 1100 – 1800 nm wavelength range.

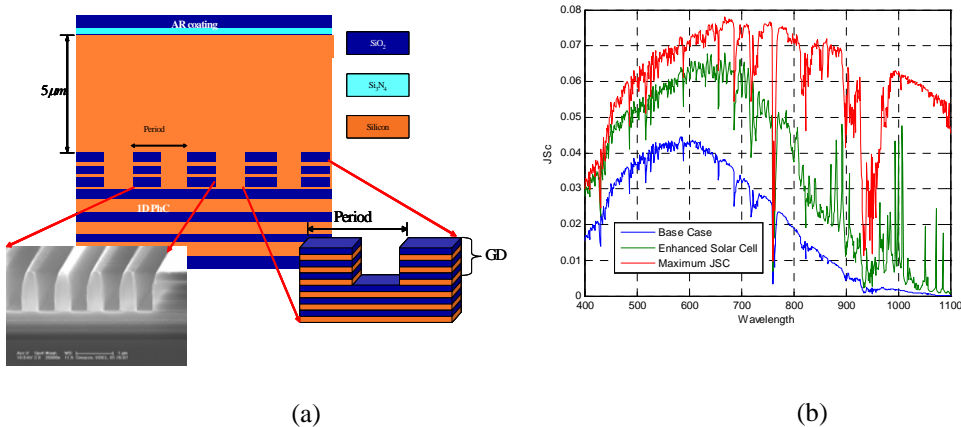


Fig. 2. (a). The cross section view of the first solar cell design with an inset SEM image of the fabricated grating and another showing an expanded view of the grating. The period of the grating is indicated and its value is 970 nm, the thickness of the layers is 128 nm for the SiO₂ layers and 218 nm for the silicon layers, the grating depth, indicated as GD is 1038 nm and there are 6 alternating layers (each alternating layer consists of a Si and SiO₂ layer) in the entire 1D PhC stack, the grating etches through the first three alternating layers, (b) simulated short circuit current of the designed structure.

The second device, as shown in Fig. 3(a) is similar to the first except that we incorporate a binary grating below the AR coating, which we fill with SiO₂, at the top surface of the cell to introduce diffraction of the incident waves; we also include a triangular grating at the bottom surface. The incorporation of a binary grating at the top of the structure introduces diffraction to the incident wave which is then subject to further redirection on encountering the triangular grating at the bottom. The combination serves to suppress lower order diffraction modes

which are present in the first device and hence further enhances performance. The optimization design parameters are similar to those of the first device with the greatest difference emerging from the introduction of the top grating and multiple periods of the triangular grating. The optimal top grating period is 260 nm and the depth is 280 nm. The alternating photonic crystal layers in the triangular grating had widths of 104 nm for the top alternating layer, 312 nm for the mid layer and 416 nm for the bottom layer of the triangle as shown in Fig. 3(a). The thickness of each of the widths in the grating is 346 nm i.e. the thickness of an alternating layer (a Si and SiO₂ layer). As with the first structure the entire 1D-PhC stack consists of six alternating layers with the first three etched through to form the grating and with three others below the grating. The resultant structure proved to be better than the first with 77 % absorption (400 – 1100 nm), a short circuit current (400 – 1100 nm) rating of 30.25 mA/cm², a band edge (867 -1100nm) enhancement factor of 4.6 and transmission of 41 % (1100 – 1800 nm).

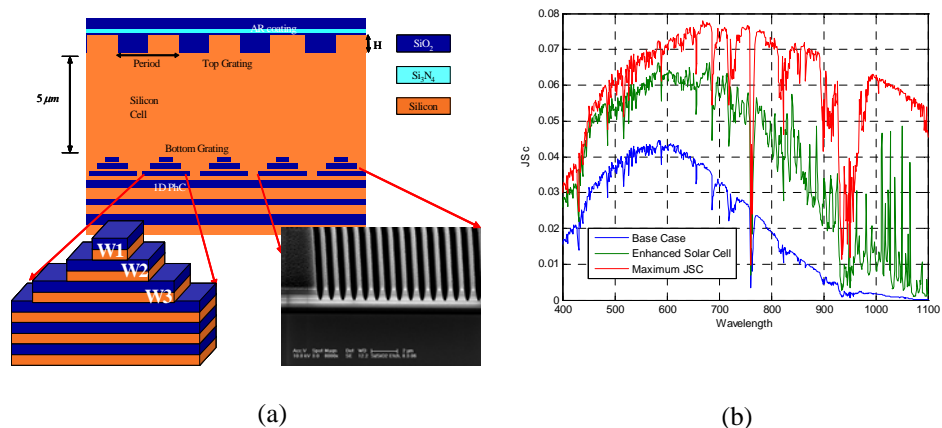


Fig. 3. (a). The cross section view of the second solar cell design with an inset SEM image of the fabricated grating and another showing an expanded view of the grating, the grating widths are indicated and the values are W1 = 104 nm, W2 = 312 nm, W3 = 416 nm, (b) the simulated short circuit current characteristics of the designed structure.

It is interesting to note the added advantage of introducing a top layer binary grating in addition to the symmetric triangular grating; we see an increase in the enhancement factor when compared to the device with only one grating at the bottom surface. Table 1 and Fig. 4. summarize the device performance of our devices when compared, in the 867 – 1100 nm range, to a silicon structure with no light trapping mechanism and one with an AR coating only.

Table 1. Enhancement factors of the different devices when compared to a device with no optical enhancements (i.e. no light trapping nor AR coating)

Structure	Enhancement Factor (867 – 1100 nm)
Silicon with no AR coating	1
Silicon with AR coating only	1.4
Device 1 (with binary grating)	3.9
Device 2 (with triangular grating)	4.6

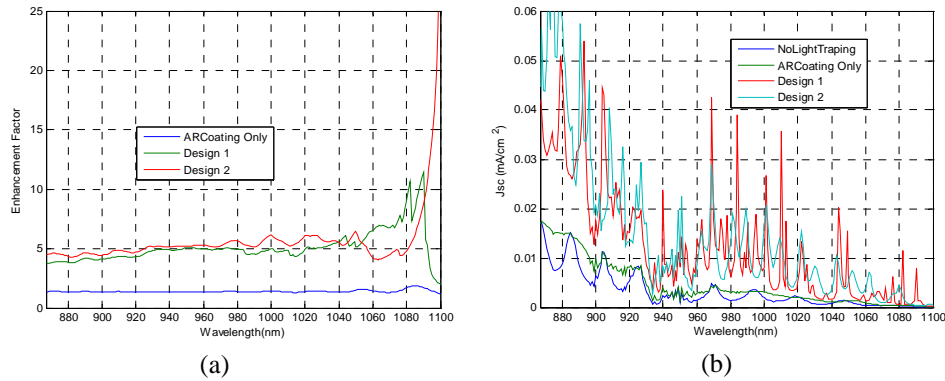


Fig. 4. (a). Enhancement factors of the different structures over the wavelength range of 867-1100nm, (b). short circuit current characteristics of the different structures over the wavelength range of 867-1800nm.

Table 2 shows the short circuit current values of the different structures and also shows the percentage enhancement of short circuit current by comparing the J_{sc} of enhanced cells to that of a structure with no light trapping or AR coating. This analysis confirms the viability of the enhanced structures as stand alone solar cells because the new devices have high short circuit current values (bandwidth considered is 400 – 1100 nm). We see that in terms of short circuit current the cell performance almost doubles when the double grating (from the second design) is applied i.e. when compared to a cell with no light trapping modifications.

Table 2. Short circuit current characteristics and Jsc enhancement of different devices when compared to a device with no optical enhancements (i.e. no light trapping or AR coating)

Structure	Jsc in mA/cm ² (400 – 1100nm)	Jsc enhancement (Percentage increase)(400 – 1100nm)
Silicon with no AR coating	15.34	N/A
Silicon with AR coating only	21.58	40.6 %
Device 1 (with binary grating)	27.4	78.5 %
Device 2 (with triangular grating)	30.25	97.2%

Diffraction gratings play a key role in the overall light trapping capabilities of our solar cell structures. In designing these gratings one has to consider three key design parameters, which are: the grating period, the duty cycle and the thickness of the grating. In our binary grating the duty cycle is fixed at 0.5. The widths of the 1D-PhC layers vary in the case of the triangular grating. The thickness of the gratings in both the binary and the triangular case are the same because they correspond to the thickness of three alternating layers of the 1D-PhC stack. However, in both cases it is important to analyze the dependence of the cell performance on the period of the gratings. Hence we model the short circuit current characteristics versus the grating period as shown in Fig. 5. We analyze grating periods greater than 500 nm because gratings with smaller periods would be more difficult to fabricate on a large scale (we consider 500 -1000 nm). The optimal binary grating period is found to be 970 nm and this corresponds to a Jsc value of 27.4 mA/cm² as shown in Fig. 5(a). For the triangular grating the optimal period is found to be 520 nm which corresponds to a Jsc value of 30.25 mA/cm² as shown in Fig. 5(b).

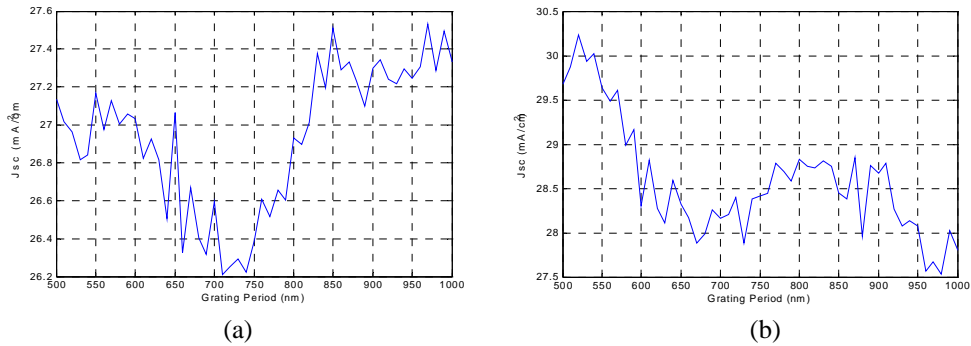


Fig. 5. (a). Effect of period on the short circuit current in the cell with a binary grating and, (b) the triangular grating cell.

We also consider the effect of variation in the incident angle on the performance of our designs. We observe only slight changes in the short circuit current characteristics as a result of the different incident angles as shown in Fig. 6. The performance of the triangular grating cell actually increases for ten and twenty degree incident angles as shown in Table 3; these results illustrate the versatility of the two designs.

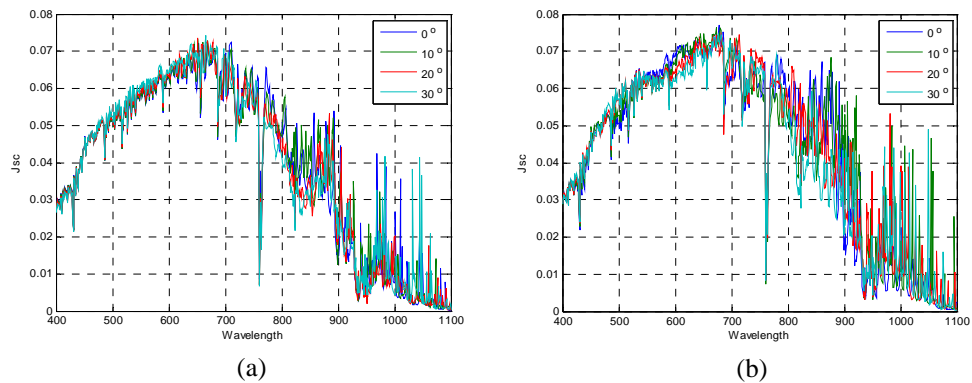


Fig. 6. (a). Dependence of cell performance on the angle of incidence of the illuminating light in the cell with a binary grating and, (b) cell with triangular grating. The different incident angles (in degrees) corresponding to the graphs are shown in the figure legends.

Table 3. Short circuit current characteristics of the two devices under illumination from light with different incident angles.

Incident Angle (in degrees)	Jsc in mA/cm ² for Device 1 (with Binary Grating)	Jsc in mA/cm ² for Device 2 (with Triangular Grating)
0	27.4	30.25
10	27.6	30.8
20	27.06	30.6
30	27.3	29.7

4. Conclusion

In this paper we have presented our design and analysis methodology for two solar cell devices. We have compared the device performance in terms of short circuit current characteristics and the enhancement factor that compares the absorption characteristics of modified device structures (with light trapping and AR coating) to those of non modified (with no light trapping) structures. The highest performance was achieved by the second design which includes two symmetric gratings, one at the top and one at the bottom of the device. This second device structure achieves a short circuit current of 30.25 mA/cm² (with normally incident light) and a band edge (867 -1100nm) enhancement factor of 4.6. We have also shown the SEM images of preliminary fabrication results of the coupled 1D-PhC and diffractive grating nano structures. Our structures achieve the design purpose of absorbing short (400 – 1100 nm) wavelengths, thus improving short circuit current characteristics, while at the same time transmitting longer (1100 – 1800 nm) wavelengths. The 1D-PhC gratings are an effective approach to light trapping in thin film solar cells and hence these structures are viable for both multiple junction and stand alone solar cells.